

Original Article

Synthesis of bi-component ZrO₂/Ag nanotube for heavy metal removal



Lee Wei Xuan¹ , Mohd Fadhil Majnis^{*1} , Syahriza Ismail² , Mohd Azam Mohd Adnan³ 

¹ Department of Chemical and Petroleum Engineering, Faculty of Engineering, Technology and Built Environment, UCSI University, Kuala Lumpur, 56000, Malaysia.

² Faculty of Manufacturing Engineering, Universiti Teknikal Malaysia Melaka, Hang Tuah Jaya, 76100 Durian Tunggal, Melaka, Malaysia.

³ Advanced Materials & Manufacturing Research Group (AMMRG), Faculty of Engineering and Life Sciences, University of Selangor, 45600 Bestari Jaya, Selangor, Malaysia.

Abstract

This study synthesised bi-component Zirconium dioxide (ZrO₂)/Silver (Ag) nanotubes through anodization and photoreduction methods. The synthesised nanotubes were characterised and adsorption tests were carried out to evaluate its performance in removing a heavy metal, lead (Pb(II)). ZrO₂ nanotubes were synthesised by anodising zirconium foil in an electrolyte composed of glycerol, ammonium fluoride, formamide, and distilled water. The effect of anodising time and the annealing process on synthesised nanotubes' morphology was studied. Bi-component ZrO₂/Ag nanotubes were prepared through photochemical reduction which silver precursor solution undergoes ultraviolet (UV) irradiation in the presence of the active reducing agent. Larger pore diameter and longer length of synthesised nanotubes were formed at the longer anodising time and the walls of nanotubes were smoother without annealing. The effect of the initial heavy metal concentration and contact time on the adsorption efficiency of synthesised nanotubes was evaluated using Pb(II) as the heavy metal ions. Overall, the percentage removal of Pb(II) increased from 10.31% to 20.31% with longer adsorption time and higher initial concentration of the Pb(II) ions.

Copyright © 2022 PENERBIT AKADEMI BARU - All rights reserved

Article Info

Received 26 October 2021

Received in revised form 21 January 2022

Accepted 29 January 2022

Available online 10 February 2022

Keywords

ZrO₂/Ag
Nanotubes
Anodization
Photoreduction
Adsorption

1 Introduction

Zirconium dioxide (ZrO₂)-based nanomaterials are nanosized metal oxides applied in heavy metal removal. Due to their high heavy metal selectivity and high removal capacity make excellent adsorbents for heavy metals in wastewater [1–3]. It has adsorption affinities towards heavy metals such as lead (Pb(II)), zinc (Zn(II)), and cadmium (Cd(II)). In previous studies, large surface areas were observed from the synthesised metal oxides and were partially composed of homogeneous nanoparticles (NPs) with crystalline cores and amorphous cells [4]. Silver (Ag) is a noble metal synthesised in nano size through various synthesis methods. Ag NPs nowadays are applied in a wide range of applications such as medical devices, home disinfectants and water purification [5]. According to Sumesh et al. [6], Ag NPs exhibit high reactivity with the mercury (II) as the reduction potential of silver reduces with the decreasing particle size, although the reactivity of mercury with bulk silver is not high.

ZrO₂ nanotubes were synthesised through anodization. Anodization involves the mechanism of the electrolytic cell in which a metal substrate is designed as an anode. It is oxidised when a constant voltage is applied to the cell system [7–9]. A few parameters manipulate the anodization process: electrolyte

* Corresponding author fadhil@ucsiversity.edu.my ✉

used, fluoride ion content in the electrolyte, voltage applied, duration of anodization, and surface modification such as annealing of synthesised nanotubes results in different components phases of zirconia nanotubes [10].

Several methods have been developed for silver doping on the surface of nanotubes, such as microwave-assisted chemical reduction method [11–13], photoreduction method [14–16], wet impregnation method [17], and in situ synthesis of Ag NPs ZrO₂ nanotubes [18,19]. The photoreduction method is simple, and it increases the possibility for desired and controllable morphology to be produced [20]. Reducing agents such as electrons, radicals, and excited species are applied to synthesise nanomaterials. Reduction of metal salts can be easily achieved and controlled through optical irradiation. The synthesis of Ag NPs in the synthesised nanotubes to be doped with is done by photochemical reduction which metal precursor solution undergoes ultraviolet (UV) irradiation in the presence of an active reducing agent. The photoreduction method enables the formation of nanoparticles in a solid-state at low temperatures. It also complies with the conclusion that desired and controllable morphology can be produced through the photoreduction method [20]. With the presence of polycarboxylic acid, spherical and rod-like nanoparticles can be obtained by controlling nanoparticles' size and shape [21].

From previous research, ZrO₂ has been proven a promising nano adsorbent in removing heavy metal ions such as lead, chromium and arsenic ions. However, the potential of advanced metal ion adsorbents in the adsorption of heavy metal ions for water purification is exciting [22]. Decoration of metallic nanoparticles onto the metal oxides has been studied, and silver (Ag) is one of the most attractive noble metals for enhancing the capability of metal oxides in eliminating the contaminants in water. For instance, enhancement of the photocatalytic activity of titanium oxide nanotubes (TNTs) under visible light in dye photodegradation [23]. However, further study is essential to elucidate the significance of noble metals in enhancing the properties of ZrO₂ for heavy metal removal. ZrO₂ nanotubes were synthesised in this study through different anodising times and annealing temperatures, then decorating Ag NPs on ZrO₂ nanotubes through the photoreduction method. SEM, EDS, and XRD characterised the synthesised bi-component ZrO₂/Ag nanotubes. The heavy metal removal performance by synthesised nanotubes was evaluated using Pb (II) as heavy metal through an adsorption test.

2 Methodology

2.1 Synthesis of ZrO₂ nanotubes

A zirconium (Zr) foil in the dimension of 10 mm × 10 mm × 0.1 mm and a carbon rod of 20 mm × 2 mm was applied as anode and cathode for the electrochemical process. Zr foil and carbon rod were pre-treated through rinsing, sonicating in acetone, ethanol, and Deionized (DI) water, and dried in the air before use. 80 mL of electrolyte composed of glycerol and formamide (volume ratio 1:1) with 1.0 wt.% NH₄F and 3.0 wt.% DI water was prepared from analytical grade chemicals. The anode and cathode were put in the prepared electrolyte, and two electrodes were kept away at 20 mm. This electrode gap ensures the formation of ZrO₂ nanotubes arrays with better morphology, large dimension and uniform ZrO₂ nanotubes [24]. 40V of potential was supplied by high-voltage direct-current potentiostat using a sweep rate of 0.1 V/s for 0.5 hours and 1 hour. Oxidation of Zr into oxide film bombarded with fluoride (F) ions provided by electrolyte was supplied with voltage to synthesise the growth of nanotubes. The ZrO₂ nanotubes were prepared to decorate Ag nanoparticles through the photoreduction method.

2.2 Decoration of Ag NPs onto ZrO₂ nanotubes

100 mL of 0.04 M AgNO₃ was added into Zr foils with thin-film ZrO₂ nanotubes and stirred well using a magnetic stirrer to achieve a ZrO₂ nanotubes/Ag mixture. The mixture was then irradiated under a UVC lamp (OSRAM, Germany) operating at 18 W and 254 nm wavelength and stirred continually for 24 hours. The product was then filtered and washed with DI water followed by a drying procedure at 100 °C for 2 hours. The synthesised ZrO₂/Ag nanotubes were then annealed at 450 °C for 3 hours.

2.3 Characterisation of ZrO₂ nanotubes

The synthesised ZrO₂ nanotubes before and after annealing and ZrO₂/Ag nanotubes were characterised with SEM to observe the morphology. EDS was used to determine the components of hybrid nanomaterials to analyse the elemental composition and ensure the composition of contaminants if any existed. The ZrO₂ nanotubes before and after annealing were also characterised by using EDS to

determine the effect of annealing and compared to ZrO₂/Ag nanotubes. The crystalline phase of ZrO₂/Ag nanotubes, ZrO₂ nanotubes before and after annealing were determined by XRD operated with Cu K α radiation at a tube current of 40 mA and voltage of 45 kV with a scan rate of 0.02 °/s over 2 θ range from 10° to 80°.

2.4 Adsorption test

Lead stock solution with (1000 mg/L) was self-prepared by dissolving 1000 mg of nitrate salts in 1 L of DI water. The solution was diluted to 200 mg/L and 600 mg/L for adsorption studies affected by initial concentration. The laboratory glassware used should be washed with 5 % v/v HNO₃ and rinsed with DI water every time after use to maintain the cleanliness of the glassware. 10 mL of lead stock solution was put in polyethylene test tubes for experiment use. The pH of the lead solution was adjusted to 6 by using HNO₃ or NaOH (0.1-0.01 mol/L concentration). Adsorption of metal ions from aqueous solutions is highly dependent on the pH of the solution, which affects the surface charge on the adsorbent and the degree of ionisation and speciation of the adsorbent. The finding by Chaouch et al. [25] indicates that Pb(II) removal is much lower at low pH could be explained by the rivalry between Pb(II) and hydrogen ions for active sites on the sorbent surface. Because the formation of soluble hydroxyl complexes limits the amount of adsorbed Pb(II) above pH = 6, and it is inferred that pH6 is the optimum value for the lead solution.

Batch adsorption was carried out in an ultrasonic bath at 53 kHz, power 100% at room temperature (25 °C). One piece of ZrO₂/Ag nanotubes foil was added into 10 mL of prepared lead solution (1000 mg/L). The mixture was agitated at 0.5 hours, 1 hour, and 1.5 hours to observe the adsorption of Pb(II) ions onto synthesised ZrO₂/Ag nanotubes. The samples were then centrifuged at 1600 rpm for 12 minutes and filtered using filter paper (grade 41). The Pb(II) concentration change was determined by using ultraviolet-visible (UV-Vis) spectroscopy. The experiment was repeated three times, and the average was obtained.

10 mg of ZrO₂/Ag nanotubes were added into different prepared lead solution concentrations (200 mg/L, 600 mg/L, and 1000 mg/L). Adsorption was carried out in an ultrasonic bath at 53 kHz, power 100 % at room temperature (25 °C) for 1 hour. The samples were then centrifuged at 1600 rpm for 12 minutes and filtered using filter paper (grade 41). The change in Pb(II) concentration was determined using UV-Vis analysis. The experiment was triplicate, and the average was obtained.

3.1 Characterisation of synthesised ZrO₂/Ag nanotubes

Fig. 1(a), 1(b), and 1(c) show the surface morphology of ZrO₂/Ag nanotubes of 0.5 hours anodization after annealing at a magnification of 30k SE(UL), 50k SE(UL) and 200k SE(UL) from a cross-sectional view. The nanotubes formed scattered in groups on the surface of the foil. Each group of nanotubes were self-arranged in a single layer with an average pore diameter of 19.8 nm. The average length of 416 nm resulted from pore and tubular structure growth on the oxide layer formed on the foil surface during anodization [26].

The dimensions of ZrO₂/Ag nanotubes were measured. The pore diameter is considerably small, and the length is short, with high voltage of 40 V applied during the anodization. It could be due to the shortened anodization hour from 3 hours to 0.5 hours. Because of the strong flow of fluoride ions caused by the high anodising voltage, a shorter anodising hour may result in less porosification of the oxide layer, increasing the electric field on the layer. As a result, after the oxide layer has porosified, the growth of nanotubes may be slowed [27]. Fig. 1(c) shows some bubble-like particles on the walls of nanotubes from the cross-sectional view. It is caused by the volume expansion of nanotubes due to a high temperature of annealing (450 °C) as the dimensions of synthesised nanotubes are smaller to withstand with 450 °C of annealing temperature [3].

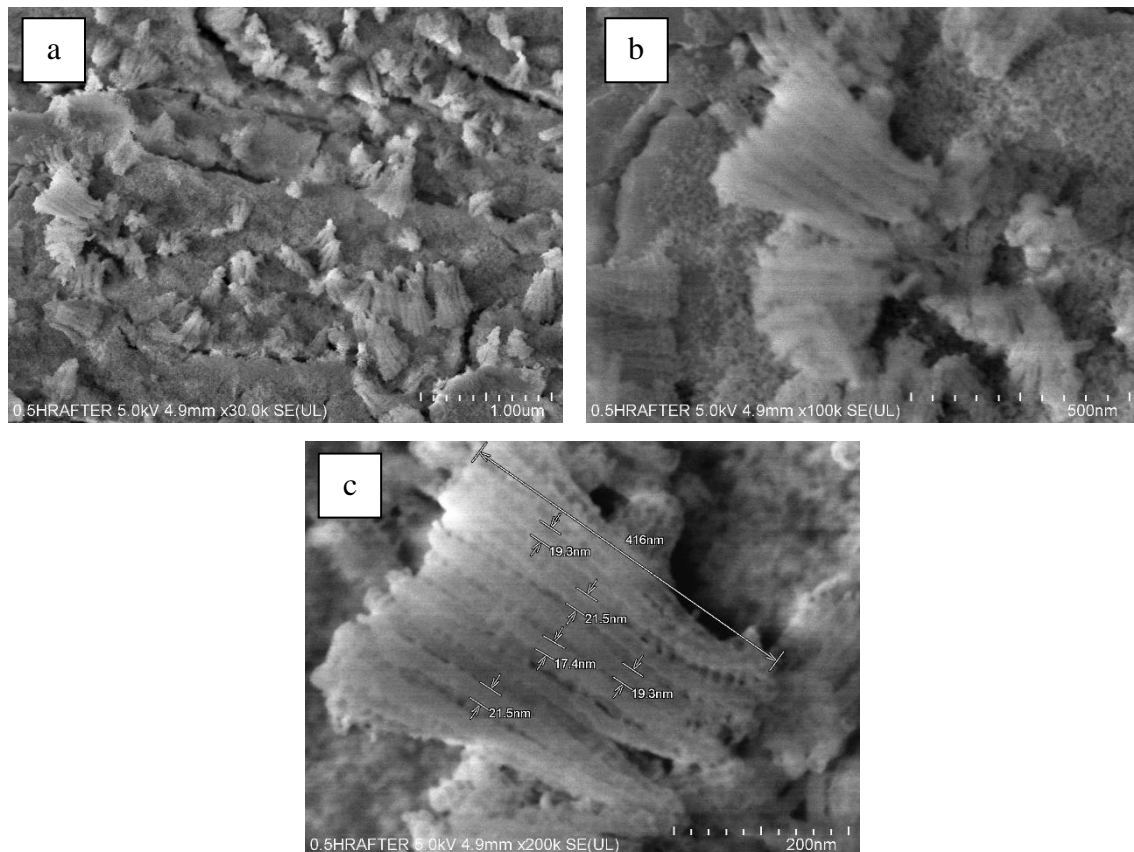


Fig. 1 Surface morphology of ZrO₂/Ag nanotubes of 0.5-hour anodization after annealing at a magnification of (a) 30k SE(UL), (b) 50k SE(UL) and (c) 200k SE(UL) from a cross-sectional view.

Fig. 2(a) and (2b) show the SEM image of non-annealed ZrO₂/Ag nanotubes anodised for 1 hour under 50k and 30k SE(UL) magnification from the top view. The nanotubes are orientated systematically, and their pores have a consistent pattern and observable pore size. Fig. 2(c) shows that the nanotubes were grown perpendicularly to the foil surface in a highly oriented pattern.

The non-annealed nanotubes anodised for 1 hour has an average length of 2.5 µm from top to bottom and an average pore diameter of 43.95 nm. The pore diameter is comparably larger than that of annealed 0.5 hours anodization nanotubes. These findings have proven the effect of anodization time on the development of nanotubes under the same voltage [10]. The nanotubes are observed to be formed in larger pore diameter and longer length under 1 hour of anodization at 40 V. There is no deterioration of nanotubes observed from the SEM images.

The SEM images of 1 hour anodization nanotubes after annealing are shown in Fig. 3(a) and 3(b) from cross-sectional view at 10k and 30k SE(UL) magnification. The nanotubes formed were ruptured and inorganized. The layers where nanotubes were formed are observed to deteriorate totally; the nanotubes are overlapped and clustered in irregular form. The dimensions of nanotubes were failed to be determined as the formation of nanotubes is not ideal, and the overlapping orientation decreases the accuracy of dimension measurement. The annealing process might cause clustered nanotubes with deteriorated tubular shape as bubble-like particles are found on the irregular nanotubes [27]. It can be concluded that the annealing temperature is too high for all the samples synthesised from Zr foil with 0.01 mm during this study.

The elemental composition of nanotubes was quantified, as shown in Fig. 4. From Fig. 4(a), 4(b) and 4(c), it is shown that the elemental composition of three of the samples includes carbon, oxide, and zirconium ions. The weight percentage (wt%) of zirconium makes up the majority wt% of the synthesised nanotubes, which is >60 wt%, followed by oxide ion, which is >30% in all samples. However, there is a minor percentage of carbon ions in two samples, 0.5 hours and 1 hour anodization nanotubes after annealing. Less than 2% of carbon impurities are found in these two samples. These

findings have proven the composition of ZrO₂ nanotubes synthesised through anodization, where an oxide layer was formed and porosified for the growth of nanotubes

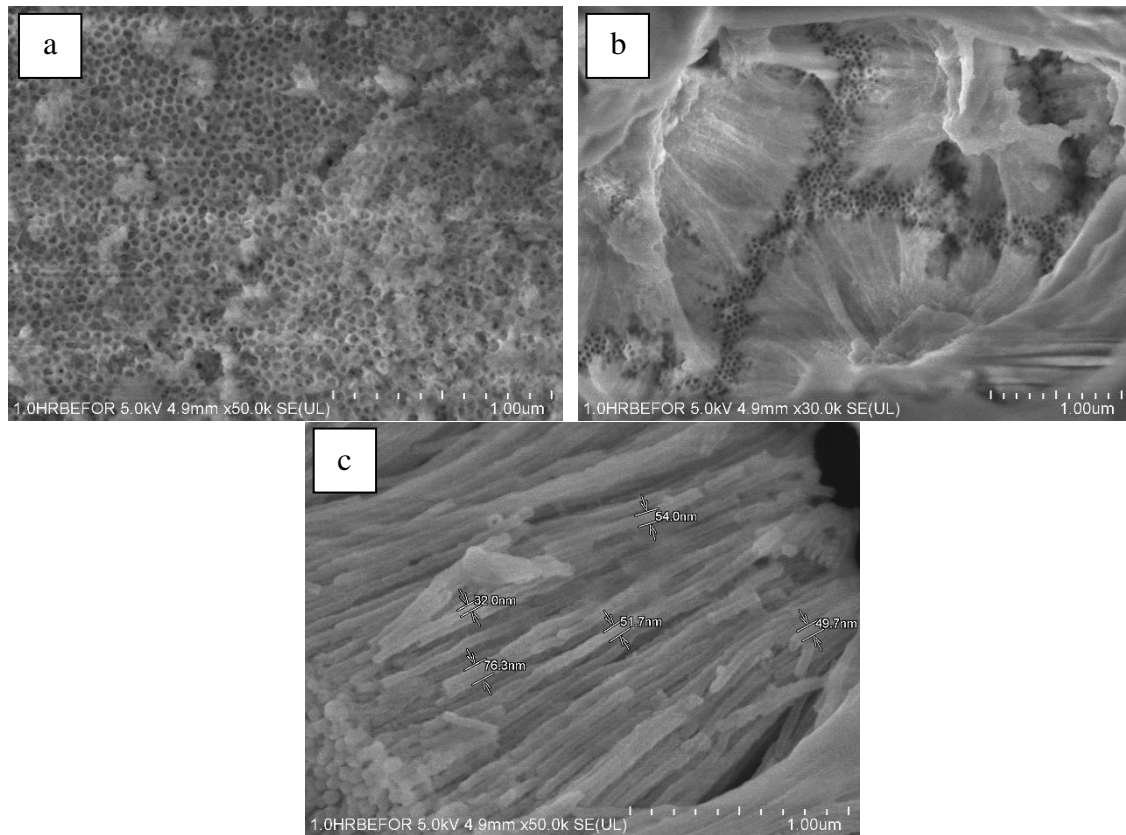


Fig. 2 SEM images of 1 hour anodization samples before annealing under (a) 50k and (b) 30k SE(UL) magnification from the top view, (c) the nanotubes were grown perpendicularly to the foil surface in a highly oriented pattern.

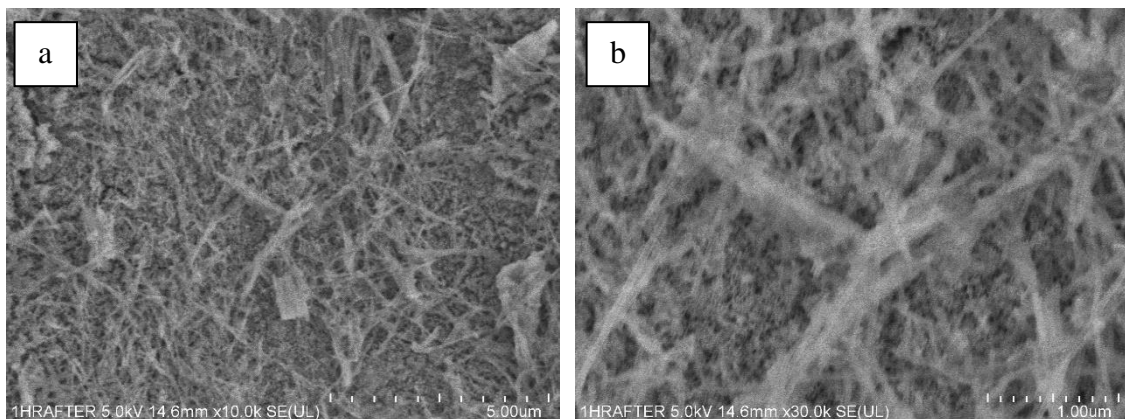


Fig. 3 SEM images of 1 hour anodization nanotubes after annealing from cross-sectional view at (a) 10k and (b) 30k SE(UL) magnification.

The carbon impurities percentage is higher, 13.38 wt%, in 1 hour anodization nanotubes before annealing as stated in Fig. 4(b). The presence of carbon might be originated from the Zr-C-O bonds, which are one of the carbonate species. Carbon impurities may have an impact on the electrical structure

of ZrO₂ nanotubes or improve the characteristics of amorphous materials [28]. There is also the presence of fluorine, 15.18 wt% in the sample. Because the samples had been in the container for more than three months, pollutants from the container or the air could have caused it. Furthermore, the fluorine could have come from the anodization electrolyte, which was made up of glycerol, ammonium fluoride, formamide, and distilled water.

Silver was absent according to the EDS elemental spectrum and quantification results of three samples. One of the reasons for the absence of silver might be the trace amount of silver in the samples, which is too small to be quantified by EDS. Besides, the unknown pressure applied might affect the photoreduction of Ag nanoparticles in ZrO₂ nanotubes. At the same time, UV light ($\lambda = 360$ nm) was being used as high pressure is required for the photoreduction of ZrO₂ nanotubes and hence the adoption of Ag nanoparticles on the reduced surface. The illumination of UV light is vital for transforming the inner surface of ZrO₂ nanotubes to be hydrophilic, which allows the solution to fill the tubes with the aid of high pressure for doping Ag nanoparticles on the surface with oxygen vacancies for the photoreduction process [29].

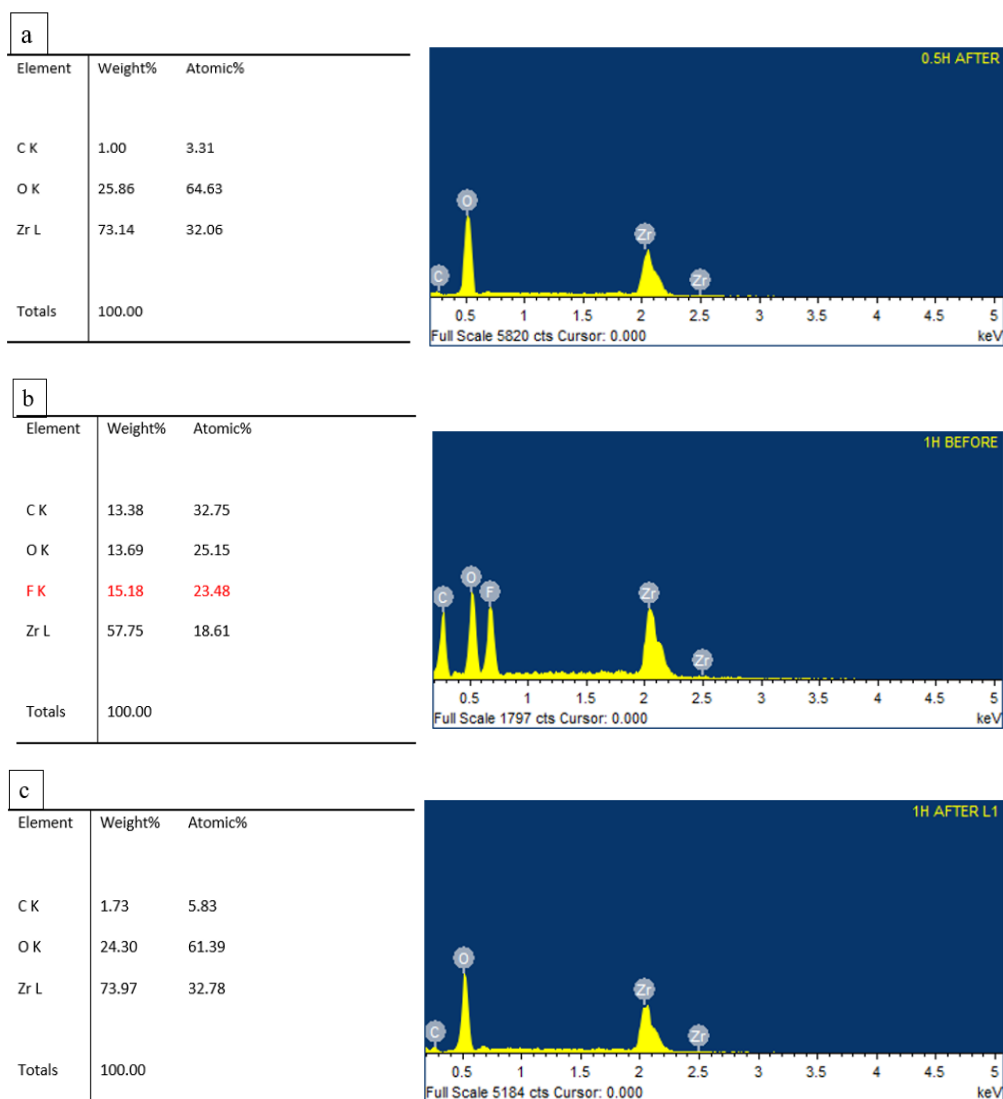


Fig. 4 EDS elemental spectrum and quantification results of (a) 0.5 hours before annealing, (b) 1 hour before annealing and (c) 1 hour after annealing.

3.2 Adsorption test results

4.5 mL of Pb(II) stock solution at different concentrations was put in a cuvette and used for curve calibration to obtain the graph with R^2 over 0.9. Light is emitted to pass through a sample at a specific wavelength in UV-Vis analysis, but not all the light will be transmitted through the sample but absorbed by it. Therefore, the transmission of light through the sample indicates the absorbance of the samples. The UV-Vis helps quantify the absorbance, and the results can be used to obtain the concentration of the related sample through graph calibration. After conducting the adsorption test at different variables, the curve obtained from UV-Vis with a specific wavelength was applied as a graph for final concentration determination. The final concentration of the adsorption test was determined by using UV-Vis, and the result was given in Absorbance (ABS). Then, the final concentration in ABS was used to determine its corresponding value in the unit of mg/L through the graph in Fig. 5. The removal percentage of Pb(II) ion was then calculated. The wavelength used in UV-Vis to determine the colourless Pb(II) ion concentration was 520 nm. The calibrated graph with corresponding Y-intercept and R^2 is shown in Fig. 5.

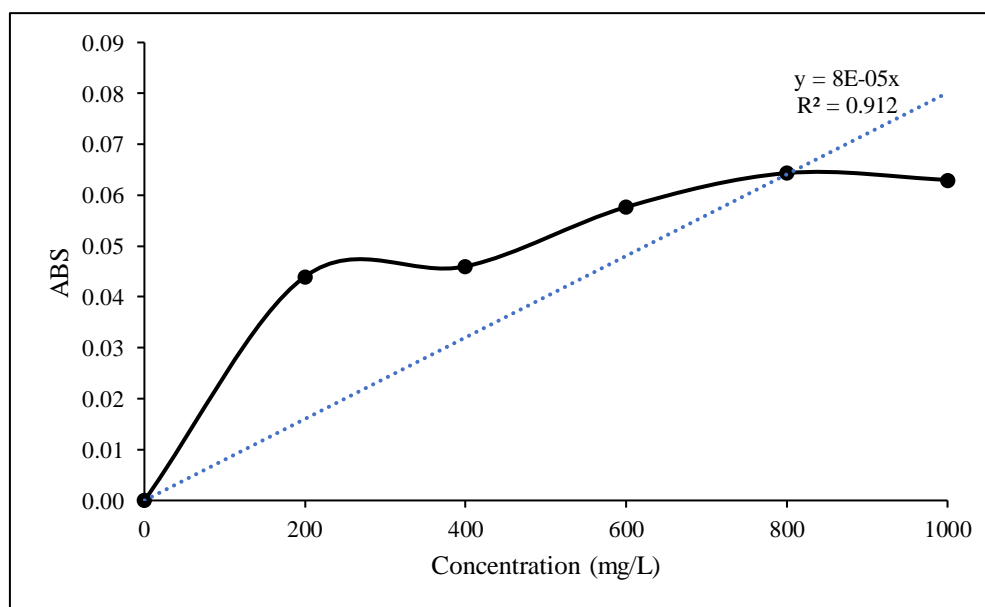


Fig. 5 ABS versus concentration (mg/L) as indicator graph of final concentration.

For the adsorption test with different contact times, 10 mL of Pb(II) stock solution of 1000 mg/L concentration and one foil of nanotubes were used. The mixture was then agitated in an ultrasonic bath at different contact times: 0.5 hours, 1 hour, and 1.5 hours with fixed pH of 6. The adsorption test was repeated for each contact time, and the average was obtained for analysis. Fig. 6 shows that the percentage removal of Pb(II) ion increases by time, 9.88%, 13.56%, and 13.91%. It is expected that the percentage removal will continue to increase with the increment of contact time. However, the Pb(II) ion removal in nanotubes will reach a saturation point that no more Pb(II) ions will be adsorbed. The final concentration of the adsorption test was initially obtained from UV-Vis in ABS. Then it was reverse calculated from the graph shown in Fig. 5 to get the corresponding final concentration.

However, it is always relatively less reliable to determine the concentration of a colourless solution by using UV-Vis, even with a specific wavelength. This condition is evident as the determination of final concentration by using UV-Vis fluctuated drastically during the adsorption test. Aside from that, the slightly defective surface structure of the synthesised nanotubes due to annealing temperature may decrease adsorption capacity as the surface of nanotubes is vital as a site for adsorption of metal ions.

For adsorption test with different initial concentrations, 200 mg/L, 600 mg/L, and 1000 mg/L and one foil of nanotubes were used for each set. The adsorption test was repeated for each different initial concentration, and the average was obtained for analysis. Fig. 7 shows that the percentage removal of

Pb(II) ion increases with the increase of initial concentration. The percentage removal of Pb(II) ion for 200 mg/L, 600 mg/L, and 1000 mg/L are correspondingly 10.31%, 14.58%, and 20.31%. The trend of the percentage removal of Pb(II) ion is positive, and it is expected that the percentage removal will continue to rise but slow down until the saturation point of nanotubes with increment in initial concentration. However, the overall efficiency of ZrO_2/Ag nanotubes in Pb(II) ion adsorption is comparatively low.

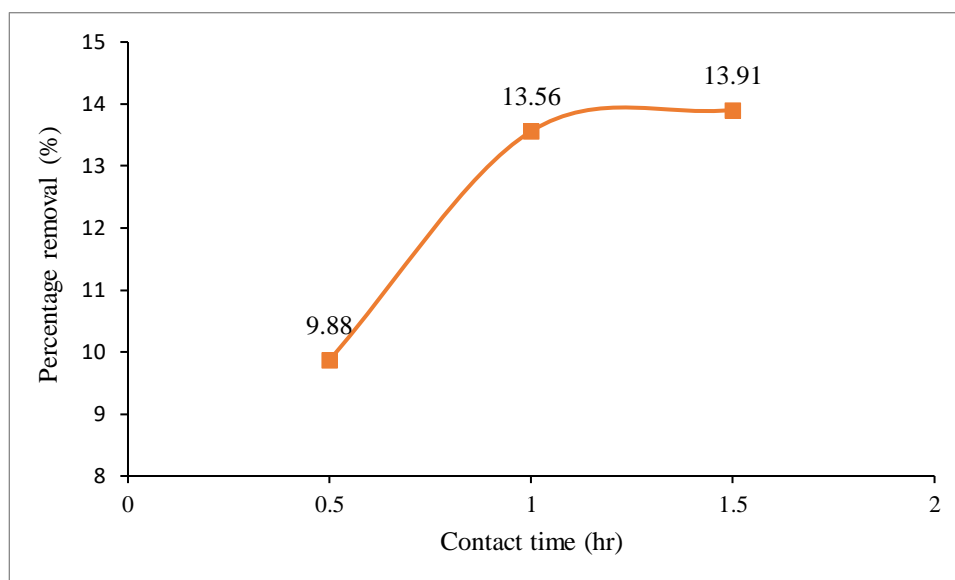


Fig. 6 Effect of contact time on Pb(II) ion percentage removal.

The unforeseen defects might significantly influence the results obtained from this adsorption test in the structure of nanotubes during the synthesis stage. This situation is evident as the ZrO_2/Ag nanotubes applied were the batch of nanotubes synthesised at 0.5 hours anodization with annealing process, which had smaller pore diameters and shorter length than that of ZrO_2 nanotubes synthesised in previous studies. The defective surface structure of the synthesised nanotubes might also contribute to the low adsorption efficiency as there was a bubble-like structure on the surface of the nanotubes, which led to irregular and rough surfaces that served as the adsorption site for heavy metal removal.

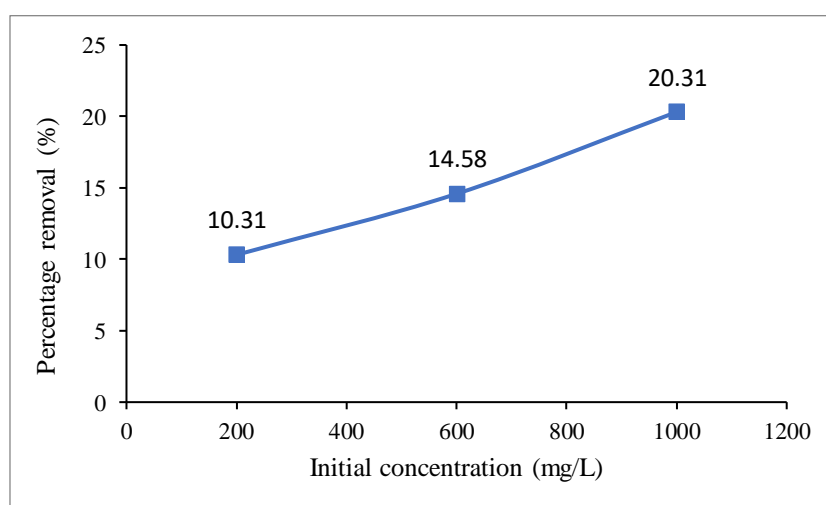


Fig. 7 Effect of initial concentration on Pb (II) ion percentage removal.

4 Conclusion

The ZrO₂/Ag nanotubes being annealed posed slightly defective properties on the surface morphology. It was observed that nanotubes with a shorter anodising period (0.5 hours) had an average pore diameter of 19.8 nm and a length of 416 nm. 1 hour anodization nanotubes before annealing had a larger pore diameter and a longer length which were 43.95 nm and 2.5 μm, respectively. The nanotubes were arranged well-ordered, with no defects observed on the nanotube walls. The annealed 1 hour anodization nanotubes were in inorganized and overlapped orientation. The tubular shape of nanotubes was deteriorated and clustered with bubble-like particles on the wall. It was found that there was Zr (>60 wt%), C (<2 wt%), and O ions (>30 wt%) in all the samples. It has proven the composition of ZrO₂ nanotubes synthesised in this study. Carbon served as an impurity in the nanotubes, but it was found lower than 2 wt%. Before annealing, carbon and fluorine impurities were found in 1 hour anodization nanotubes, 13.38 wt% and 15.18 wt%, respectively. Ag nanoparticles were unable to be detected in all the samples. Hence the synthesised nanotubes were pure ZrO₂ nanotubes. The maximum percentage of heavy metal removed by annealed 0.5 hours anodization nanotubes was 13.91%, which increased as contact time increased. Furthermore, the proportion of heavy metal removed rose with the increase in starting concentration, reaching a maximum of 20.31%. Therefore, the synthesised nanotubes were applicable in heavy metal removal through adsorption.

Acknowledgement

We acknowledge the support of time, materials and facilities from UCSI University (Centre of Excellence for Research, Value Innovative and Entrepreneurship (CERVIE), UCSI University Proj-In-FETBE-056), Selangor Research Grant (GPNS-01/UNISEL/18-047), Universiti Selangor (UNISEL) and Universiti Teknikal Malaysia Melaka for this study.

Declaration of Conflict of Interest

The authors declared that there is no conflict of interest with any other party on the publication of the current work.

ORCID

Lee Wei Xuan  <https://orcid.org/0000-0002-3416-7277>

Mohd Fadhil Majnis  <https://orcid.org/0000-0001-8477-1272>

Syahriza Ismail  <https://orcid.org/0000-0003-3448-7649>

Mohd Azam Mohd Adnan  <https://orcid.org/0000-0003-0348-7291>

References

- [1] K. Gupta, P. Joshi, R. Gusain, O.P. Khatri, Recent advances in adsorptive removal of heavy metal and metalloid ions by metal oxide-based nanomaterial, *Coordination Chemistry Reviews* 445 (2021) 214100. <https://doi.org/10.1016/j.ccr.2021.214100>.
- [2] A.M. Awad, R. Jalab, A. Benamor, M.S. Nasser, M.M. Ba-Abbad, M. El-Naas, A.W. Mohammad, Adsorption of organic pollutants by nanomaterial-based adsorbents: An overview, *Journal of Molecular Liquids* 301 (2020) 112335. <https://doi.org/10.1016/j.molliq.2019.112335>.
- [3] J. Liu, Z. Zhao, C. Xu, J. Liu, Structure, synthesis, and catalytic properties of nanosize cerium-zirconium-based solid solutions in environmental catalysis, *Chinese Journal of Catalysis* 40(10) (2019) 1438–1487. [http://dx.doi.org/10.1016/S1872-2067\(19\)63400-5](http://dx.doi.org/10.1016/S1872-2067(19)63400-5).
- [4] J. Yang, B. Hou, J. Wang, B. Tian, J. Bi, N. Wang, X. Lin, X. Huang, Nanomaterials for the removal of heavy metals from wastewater *Nanomaterials* 9(3) (2019). <https://doi.org/10.3390/nano9030424>.
- [5] N.X. Dinh, D.T. Chi, N.T. Lan, H. Lan, H.V. Tuan, N.V. Quy, V.N. Phan, T.Q. Huy, A. Le, Water-dispersible silver nanoparticles-decorated carbon nanomaterials: synthesis and enhanced antibacterial activity, *Applied Physics A: Materials Science and Processing* 119(1) (2015) 85–95. <https://doi.org/10.1007/s00339-014-8962-6>.
- [6] E. Sumesh, M.S. Bootharaju, Anshup, T. Pradeep, A practical silver nanoparticle-based adsorbent for the removal of Hg²⁺ from water, *Journal of Hazardous Materials*, 189(1–2) (2011) 450–457. <https://doi.org/10.1016/j.jhazmat.2011.02.061>.
- [7] T. Wen, H. Tan, S. Chen, P. He, S. Yang, C. Deng, and S. Liu, Growth behavior of tantalum oxide

- nanotubes during constant current anodization, *Electrochemistry Communications* 128 (2021) 107073. <https://doi.org/10.1016/j.elecom.2021.107073>.
- [8] Y. Ni, J. Zhang, T. Gong, M. Sun, Z. Zhao, X. Li, H. Yu, X. Zhu, Quantitative analysis of the volume expansion of nanotubes during constant voltage anodization, *Surfaces and Interfaces*, 26 (2021) 101419. <https://doi.org/10.1016/j.surfin.2021.101419>.
- [9] M.S.A. Berahim, M.F. Majnis, M.A.A. Taib, Formation of titanium dioxide nanoparticles by anodization of valve metals, *Progress in Energy and Environment* 7 (2019) 11–19. <https://www.akademiabaru.com/submit/index.php/progee/article/view/1050>.
- [10] M. D. L. Balela, C. Mancera, B. P. Reyes, M.C. Reyes, Anodization of zirconia nanotubes for lead (II) adsorption, *Materials Science Forum*, 939 (2018) 113–119. <https://doi.org/10.4028/www.scientific.net/MSF.939.113>.
- [11] M. Shkir, M. T. Khan, I. M. Ashraf, S. AlFaify, A.M. El-Toni, A. Aldalbahi, H. Ghaithan, A. Khan, Rapid microwave-assisted synthesis of Ag-doped PbS nanoparticles for optoelectronic applications, *Ceramics International* 45(17) (2019) 21975–21985. <https://doi.org/10.1016/j.ceramint.2019.07.212>.
- [12] N. Thakur, Anu, K. Kumar, Effect of (Ag, Co) co-doping on the structural and antibacterial efficiency of CuO nanoparticles: A rapid microwave assisted method, *Journal of Environmental Chemical Engineering* 8(4) (2020) 1–9. <https://doi.org/10.1016/j.jece.2020.104011>.
- [13] U. Kamran, S.J. Park, Microwave-assisted acid functionalized carbon nanofibers decorated with Mn doped TNTs nanocomposites: Efficient contenders for lithium adsorption and recovery from aqueous media, *Journal of Industrial and Engineering Chemistry*, 92 (2020) 263–277. <https://doi.org/10.1016/j.jiec.2020.09.014>.
- [14] M.Z. Toe, A.T. Le, S.S. Han, K.A.B. Yaacob, S.Y. Pung, Silver nanoparticles coupled ZnO nanorods array prepared using photo-reduction method for localized surface plasmonic effect study, *Journal of Crystal Growth* 547 (2020) 125806. <https://doi.org/10.1016/j.jcrysgro.2020.125806>.
- [15] F. Lu, J. Wang, Z. Chang, J. Zeng, Uniform deposition of Ag nanoparticles on ZnO nanorod arrays grown on polyimide/Ag nanofibers by electrospinning, hydrothermal, and photoreduction processes, *Materials and Design* 181 (2019) 108069. <https://doi.org/10.1016/j.matdes.2019.108069>.
- [16] M. Jodeyri, M. Haghighi, M. Shabani, Plasmon-assisted demolition of antibiotic using sono-photoreduction decoration of Ag on 2D C₃N₄ nanophotocatalyst enhanced with acid-treated clinoptilolite, *Ultrasonics Sonochemistry* 54 (2019) 220–232. <https://doi.org/10.1016/j.ultsonch.2019.01.035>.
- [17] R. Gupta, N.K.R. Eswar, J.M. Modak, G. Madras, Ag and CuO impregnated on Fe doped ZnO for bacterial inactivation under visible light, *Catalysis Today* 300 (2018) 71–80. <http://dx.doi.org/10.1016/j.cattod.2017.05.032>.
- [18] L. Zhou, J. Yang, X. Wang, G. Song, F. Lu, L. You, J. Li, Ag nanoparticles decorated Ag@ZrO₂ composite nanospheres as highly active SERS substrates for quantitative detection of hexavalent chromium in waste water, *Journal of Molecular Liquids* 319 (2020) 114158. <https://doi.org/10.1016/j.molliq.2020.114158>.
- [19] M. Maham, M. Nasrollahzadeh, S. Mohammad Sajadi, Facile synthesis of Ag/ZrO₂ nanocomposite as a recyclable catalyst for the treatment of environmental pollutants, *Composites Part B: Engineering* 185 (2020) 107783. <https://doi.org/10.1016/j.compositesb.2020.107783>.
- [20] P. Rajapandiyar, J. Yang, Photochemical method for decoration of silver nanoparticles on filter paper substrate for SERS application, *Journal of Raman Spectroscopy* 45(7) (2014) 574–580. <https://doi.org/10.1002/jrs.4502>.
- [21] S.Z. Qiao, J. Liu, G.Q. Max Lu, *Synthetic Chemistry of Nanomaterials. Modern Inorganic Synthetic Chemistry*, Second Edition, Elsevier B.V., 2017. <http://dx.doi.org/10.1016/B978-0-444-63591-4.00021-5>
- [22] V.R. Dandu Kamakshi Gari, M. Kim, Removal of Pb(II) using silver nanoparticles deposited graphene oxide: equilibrium and kinetic studies, *Monatshefte fur Chemie* 146(9) (2015) 1445–1453. <https://doi.org/10.1007/s00706-015-1429-4>.
- [23] P. Van Viet, B. Thang Phan, D. Mott, S. Maenosono, T. Tan Sang, C. Minh Thi, L. Van Hieu, Silver nanoparticle loaded TiO₂ nanotubes with high photocatalytic and antibacterial activity synthesized by photoreduction method, *Journal of Photochemistry and Photobiology A: Chemistry* 352 (2018) 106–112. <https://doi.org/10.1016/j.jphotochem.2017.10.051>.
- [24] M. Wang, L. Jia, and S. Deng, Influence of anode area and electrode gap on the morphology of TiO₂ nanotubes arrays 534042 (2013). <https://doi.org/10.1155/2013/534042>.
- [25] N. Chaouch, M.R. Ouahrani, S.E. Laouini, Adsorption of Lead (II) from aqueous solutions onto activated carbon prepared from algerian dates stones of phoenix dactylifera L (Ghars variety) by H₃PO₄ activation, *Oriental Journal of Chemistry* 30(3) (2014) 1317–1322. <http://dx.doi.org/10.13005/ojc/300349>
- [26] K. Yasuda, P. Schmuki, Formation of self-organized zirconium titanate nanotube layers by alloy anodization, *Advanced Materials* 19(13) (2007) 1757–1760. <https://doi.org/10.1002/adma.200601912>.
- [27] L. Guo, J. Zhao, X. Wang, X. Xu, H. Liu, Y. Li, Structure and bioactivity of zirconia nanotube arrays

- fabricated by anodization, *International Journal of Applied Ceramic Technology* 6(5) (2009) 636–641. <https://doi.org/10.1111/j.1744-7402.2008.02305.x>.
- [28] N. Bashrom, K.A. Razak, C.K. Yew, Z. Lockman, Effect of Fluoride or Chloride ions on the morphology of ZrO_2 thin film grown in ethylene glycol electrolyte by anodization, *Procedia Chemistry* 19 (2016) 611–618. <http://dx.doi.org/10.1016/j.proche.2016.03.060>.
- [29] X. Pan, M.Q. Yang, X. Fu, N. Zhang, Y.J. Xu, Defective TiO_2 with oxygen vacancies: Synthesis, properties and photocatalytic applications, *Nanoscale* 5(9) (2013) 3601–3614. <https://doi.org/10.1039/C3NR00476G>.